Colloid Polym Sci (2008) 286:941–949
DOI 10.1007/s00396-008-1852-8

ORIGINAL CONTRIBUTION

Sedimentation and drying dissipative patterns of ternary mixtures of colloidal silica spheres having different sizes

Tsuneo Okubo · Junichi Okamoto · Akira Tsuchida

Received: 8 January 2008 / Revised: 10 February 2008 / Accepted: 16 February 2008 / Published online: 12 March 2008

Abstract The sedimentation and drying dissipative structural patterns were formed during the course of drying ternary mixtures of colloidal silica spheres of 183 nm, 305 nm, and 1.205 μm in diameter in aqueous suspension on a watch glass, a glass dish, and a cover glass. The patterns were observed by closed-up pictures, metallurgical optical microscopy, 3D profile microscopy, reflection spectroscopy and AFM images. The concentrations of the three spheres ranged from 0.0023 to 0.0128 keeping the same concentrations for each spheres. Broad ring-like sedimentation patterns were formed within a short time in suspension state especially in a glass dish. In a watch glass, colorful three layered ring-like drying patterns were observed and composed of the outer, middle and inner layers of small, medium, and large spheres, respectively. The three colored segregated layers were formed by the balancing between the outward convectional flow and the inward sedimentation of spheres. In a glass dish, wave-like macroscopic drying patterns were observed in the intermediate areas between the outside edge of the broad ring at the central area and the inner wall of the cell especially at low sphere concentrations. The size of the broad ring at the central area increased as sphere concentration increased. On a cover glass, size segregation also took place, i.e., small, medium, and large spheres located at the outer, medium, and central areas, though these segregations were not so complete compared with those on a watch glass.

Keywords Sedimentation dissipative structure · Drying dissipative structure · Segregation · Colloidal silica spheres · Ternary mixtures · Broad ring pattern · Wave-like pattern

T. Okubo (✉)
Institute for Colloidal Organization,
Hatoyama 3-1-112,
Uji, Kyoto 611-0012, Japan
e-mail: okubotsu@ybb.ne.jp

T. Okubo
Cooperative Research Center, Yamagata University,
Johnan 4-3-16,
Yonezawa 992-8510, Japan

J. Okamoto · A. Tsuchida
Department of Applied Chemistry, Gifu University,
Gifu 501-1193, Japan

Introduction

Most structural patterns in nature are formed via self-organization accompanied with the dissipation of free energy and in the non-equilibrium state. Among several factors in the free energy dissipation of aqueous colloidal suspensions, evaporation of solvent molecules at the air–solvent interface and the gravitational convection are very important. In order to understand the mechanisms of the dissipative self-organization of the simple model systems, instead of complex nature itself, several research groups including us have studied the *convectional* [1–7], *sedimentation* [8–12], and *drying* dissipative patterns in the course of drying of suspensions and solutions [13–48].

In a previous work [48], sedimentation and drying dissipative patterns of the binary mixtures among the colloidal silica spheres, 183 nm, 305 nm, and 1.205 μm in diameter, were studied on a watch glass, a glass dish, and a cover glass in the macroscopic and microscopic scales. In a watch glass, macroscopic drying patterns were composed of the outer and inner layers of small and large spheres, respectively. The two colored layers were ascribed to the Bragg diffraction of light by the dried colloidal crystals of the corresponding spheres. The width ratio of the layers

changed in proportion to the mixing ratio of each spheres. Furthermore, on a cover glass, the sphere-mixing ratios were analyzed from the widths of the drying broad rings of the small spheres at the outside edge. High and distinct broad rings of small spheres and low and vague broad rings formed at the outside edge and in the inner area, respectively. Drying dissipative pattern was clarified to be one of the novel analysis techniques of colloidal size in the binary colloidal mixtures.

In this work, we extended our study on the ternary mixtures of the colloidal silica spheres, 183 nm, 305 nm, and 1.205 μm in diameter in order to know how precisely the size segregation takes place in the drying dissipative patterns. The concentrations of the three spheres in this work ranged from 0.0023 to 0.0128, keeping the same concentrations for each sphere.

Experimental

Materials

CS161, CS300, and CS1000A silica spheres were kindly donated from Catalysts & Chemicals Ind. Co. (Tokyo). Diameters, standard deviations from the mean diameter and polydispersity indices of the spheres were 183 nm±18.6 nm and 0.10, 305 nm±9.1 nm and 0.030, and 1.205 μm± 14 nm and 0.012, respectively. These size parameters were determined from an electron microscope (Hitachi, H8100) in Gifu University. The CS300 and CS1000A spheres were carefully purified by repeated decantation more than thirty times. Then the samples including CS161 were treated on a mixed bed of cation- and anion-exchange resins [Bio-Rad, AG501-X8(D), 20–50 mesh] more than 6 years before use, since newly produced silica spheres always release a considerable amount of alkali ions from the porous sphere surfaces for a long time. Water used for the sample preparation was purified by a Milli-Q reagent grade system (Milli-RO5 plus and Milli-Q plus, Millipore, Bedford, MA).

Observation of the dissipative structures

Aqueous suspensions of the silica samples measuring 4 ml, 5 ml, or 0.1 ml were put carefully and gently into a medium size watch glass (70 mm in diameter, TOP Co. Tokyo), a glass dish (42 mm in inner diameter and 15 mm in height, code 305-02, TOP Co., Tokyo) or a cover glass (30 mm× 30 mm, thickness No. 1, 0.12 to 0.17 mm, Matsunami Glass Co., Kishiwada, Osaka) set in a glass dish (60 mm in diameter, 15 mm in depth, Petri Co., Tokyo), respectively. The sedimentation and drying patterns were observed for the suspensions on a desk covered with a black plastic sheet until it dried up completely in an air-conditioned room at 24±1 °C. The humidity of the room air was between 45–60%, which was not regulated in our experiments. The concentrations of the ternary components were kept to be the same, and were 0.00229, 0.0046, 0.0069, and 0.0128 in volume fraction. Thus, the mixing ratio of the three sphere components was kept uniform for each suspension. It should be mentioned here that the dried state of the film was checked from the reflection spectroscopy, where the peak profiles did not change with time. Furthermore, observation of the drying processes was made on/in the substrate without cap in the present work. Thus, the contamination of carbon dioxide in air must be considered as a whole in the experimental period, especially at the low sphere concentrations. However, the contamination effect will be rather small, since sample suspension is always concentrated during the course of dryness.

Macroscopic dissipative structures were observed on a Canon EOS 10D digital camera (Canon Co., Tokyo) with a lens (EF 28–200 mm, f=3.5–5.6 USM, Canon). Microscopic structures were observed with a metallurgical microscope (PME-3, Olympus Co., Tokyo). Thickness profiles of the dried films were measured on a laser 3D profile microscope (type VK-8500, Keyence Co., Osaka). Reflection spectra of the dried film were recorded on a high-sensitivity spectrum multi-channel photo-detector (MCPD-7000 G3, Otsuka Electronics, Osaka) with a Y-type optical fiber. AFM (Atomic Force Microscopy) measurements were made on a nano-scale hybrid microscope (type VN-8000, Keyence).

Results and discussion

Macroscopic sedimentation and drying patterns of ternary sphere mixtures

Figure 1 shows the sedimentation (a to c, e to g and i to k) and drying patterns (d, h and l) of ternary sphere mixtures in a watch glass, a glass dish and a cover glass, respectively. In a watch glass, sedimentation took place within 25 min after the suspensions were set, and the two layers (white and blue) at least were formed in the liquid area after 20 h and 35 min. Interestingly, the drying pattern shown in Fig. 1d is composed of three layers, whitish, greenish, and bluish ones, from the center to the outside edge. These three different colored layered patterns support occurrence of the size segregation during the course of dryness.

In a glass dish, broad ring patterns were observed within 30 min for the suspension phase, and the suspensions dried up after 4.2 days. It should be recalled that the broad ring

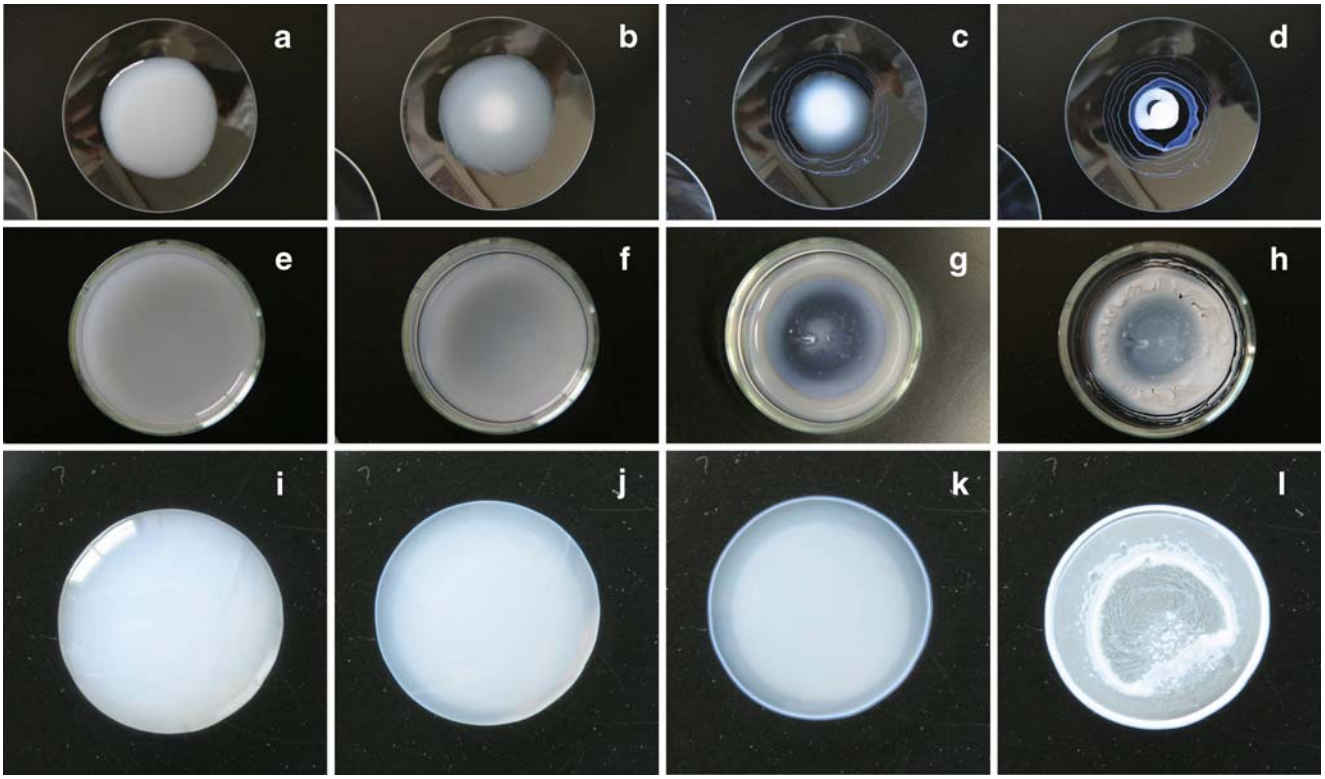

Fig. 1 Sedimentation and drying patterns of CS1000A (component 1)+CS300 (2)+CS161 (3) mixtures in a watch glass (4 ml, **a** after 25 min, **b** 5 h 10 min, **c** 20 h 35 min, **d** 28 h 5 min, dry), a glass dish (**e** after 30 min, **f** 72 h 20 min, **g** 82 h 50 min, **h** 100 h 50 min, dry) and a cover glass (**i** after 30 min, **j** 2 h 30 min, **k** 3 h 25 min, **l** 4 h 45 min, dry) at 24 °C. $\phi_1=\phi_2=\phi_3=0.0069$

patterns did not appear at all in a dish with cap for colloidal silica spheres, 1.2 μm [8], 560 nm [12], and 300 nm in diameter [11]. It should be noted that the broad rings formed rather quickly several minutes after suspension was set and in the stage of the incomplete sedimentation of spheres, which shows the convectional flow of water and spheres are vigorous even at room temperature.

A main cause for the broad ring formation is due to the convectional flow of water and colloidal silica spheres in the different rates, where the rate of water will be slower than that of the colloidal spheres under gravity. Especially, flow of the spheres from the central area toward the outside edge in the lower layer of the liquid, which was observed directly from the movement of the reversibly occurred aggregates of the colloidal particles of Chinese black ink [5] and also poly (methyl methacrylate) spheres [Okubo T, Okamoto J, Tsuchida A, publication in preparation], is important. Clearly, the convectional flow is enhanced by the evaporation of water at the liquid surface, resulting in the lowering of the suspension temperature in the upper region of the suspension. The magnitudes of the temperature lowering at the liquid surface at 25 °C compared with the bulk temperature were estimated to be 2 and 1.5 °C at 40% and 80% air humidity, respectively, and those at 40 °C were 5 °C and 2 °C, respectively [49, 50]. When the colloidal spheres reach the edge wall of the dish at the outside region of the liquid, a part of the spheres will turn to upward and go back to the center region. However, most spheres may drop downward on the cell bottom close to the outside cell wall, where the effective horizontal flow of the spheres may stop temporarily. This process must be followed by the broad ring accumulation of the spheres near the round outside edges. It should be noted that the convectional flow rates should increase as the sphere size decreases. It is highly plausible that the broad ring is composed of three different rings corresponding to the sizes of the ternary spheres. However, experimental errors were larger than the magnitude of the segregation of the broad rings. This will be discussed again later in the "Microscopic drying patterns of ternary sphere mixtures" section. It should be noted here that the broad ring-like sedimentation patterns in the liquid phase reported here were observed first in a previous paper from the author's laboratory [9] as the author knows. However, the broad ring formation in the dried film has been observed so often for most of the solutions and suspensions examined by our group [5–12, 33–49] and further by other researchers [13–32].

Figures 1i to 1 show the sedimentation and drying patterns of ternary sphere mixtures on a cover glass. The liquid's shape is round hill and recognition of the broad ring

is rather difficult with the naked eyes in the suspension state. However, the clear-cut broad rings observed in the drying pattern support that the broad rings should be formed already in the sedimentation patterns (Fig. 1i and k). It should be noted that the clear-cut broad ring observed in Fig. 1k at the outside edge is the dried pattern and not in the liquid phase. The drying pattern (Fig. 1l) shows the broad ring was formed also in the middle area. However, the size-segregated patterns were not observed clearly on the macroscopic scale.

Figure 2 shows the typical examples of the sedimentation patterns of the ternary mixtures at the different concentrations of spheres from $\phi_1=\phi_2=\phi_3=0.00229$ to 0.0128 in a watch glass, a glass dish, and a cover glass, respectively. These patterns of the ternary mixtures are similar irrespective of the total sphere concentration, though the patterns at low sphere concentration look clearer with the naked eyes. The sedimentation broad ring patterns of the ternary mixtures are also similar to those of the corresponding single component suspensions. It should be mentioned here that sharpness of the sedimentation broad rings in a glass dish was sensitive to the change in the room temperature and/or humidity, though the pictures showing this were omitted in this report. This finding has been reported in a previous work for the first time [15]. It is highly plausible that the sedimentary spheres are surrounded with the extended electrical double layers and float and move along the cell plate, which is also surrounded by the electrical double layers, under the influence of the convectional flow of water.

Figure 3 shows the drying patterns of the ternary mixtures of CS1000A (component 1)+CS300 (2)+CS161 (3) at four different sphere concentrations at the condition of $\phi_1=\phi_2=\phi_3$ in a watch glass (a to d), a glass dish (e to h) and a cover glass (i to l), respectively. In Fig. 3d, the three different colored layers (white, green, and blue) are formed from the center to the outside regions, respectively. These drying pattern supports that the patterns of the ternary mixtures are composed of the inner layer of large spheres, middle layer of middle spheres and the outer layer of small spheres. This size-segregation effect for the ternary mixtures was supported also from the reflection spectroscopy in a watch glass, which will be discussed below in the "Microscopic drying patterns of ternary sphere mixtures" section. For the ternary mixtures at low concentrations, however, distinct three layers were not recognized with the naked eyes in the drying patterns in a watch glass (see Fig. 3a to c), though two layers of the inner white and outer blue were clearly observed. It should be recalled here that the rather sharp size-segregation effect in a watch glass compared with those on other substrates is due to the effective balancing between upward (or outward) convec-

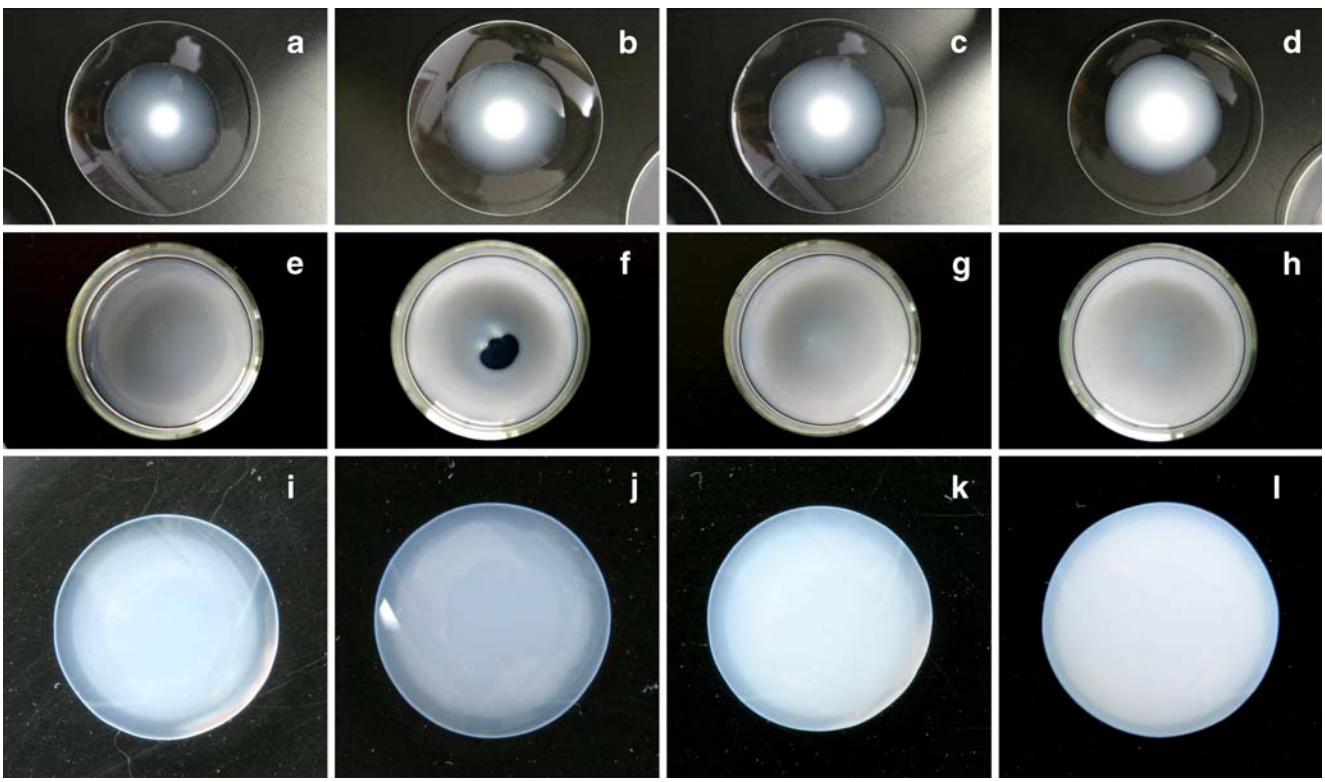

Fig. 2 Sedimentation patterns of CS1000A (1)+CS300 (2)+CS161 (3) mixtures in a watch glass (after 9 h 50 min), a glass dish (after 76 h 15 min), and a cover glass (after 2 h 30 min) at 24 °C. **a**, **e**, **i** $\phi_1=\phi_2=\phi_3=0.00229$, **b**, **f**, **j** 0.0046, **c**, **g**, **k** 0.0069, **d**, **h**, **l** 0.0128

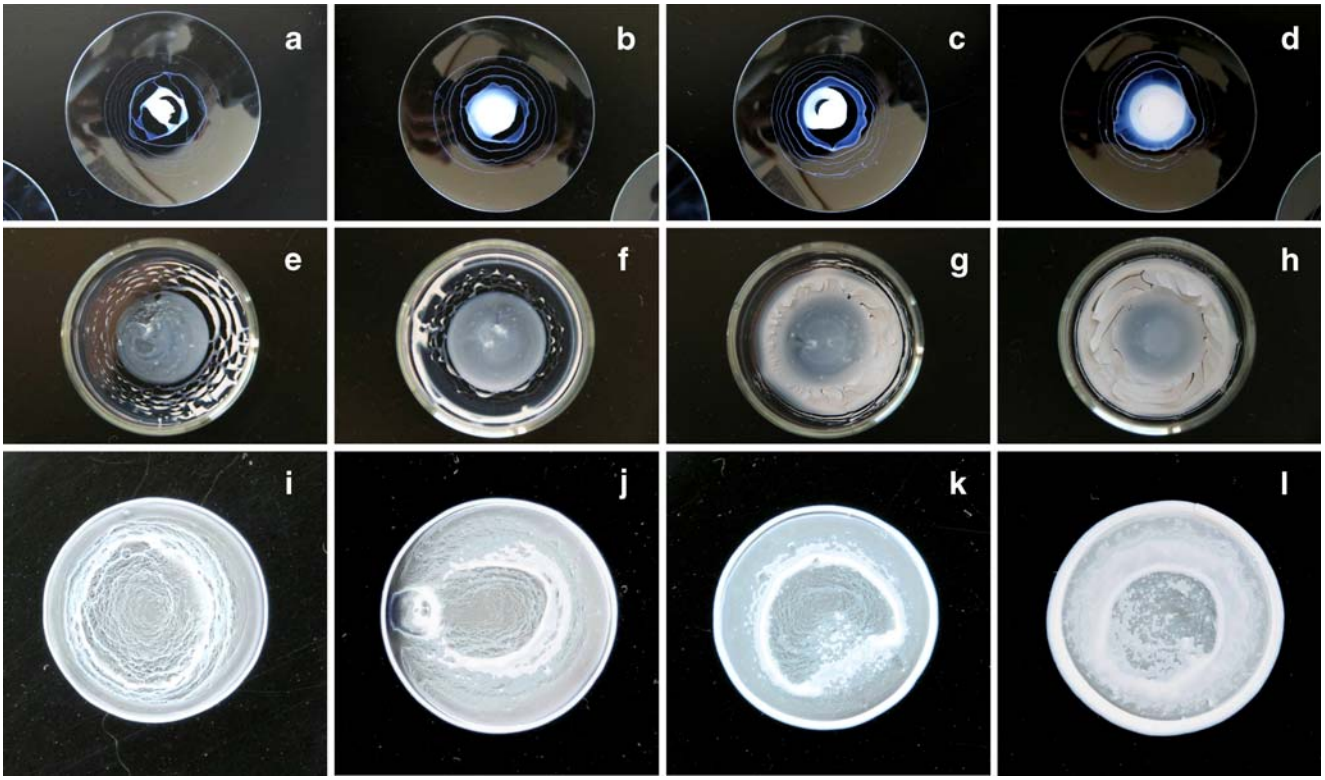

Fig. 3 Drying patterns of CS1000A (1)+CS300 (2)+CS161 (3) mixtures in a watch glass (after 28 h 5 min), a glass dish (after 100 h 50 min), and a cover glass (after 4 h 45 min) at 24 °C. **a**, **e**, **i** $\phi_1=\phi_2=\phi_3=0.00229$, **b**, **f**, **j** 0.0046, **c**, **g**, **k** 0.0069, **d**, **h**, **l** 0.0128

tional flow and the downward (or inward) sedimentation of spheres [48]. Small spheres move upward fast by the convectional flow and also move downward slowly by the sedimentation compared with large spheres.

The wave-shaped and slightly iridescent colored structures were formed in the intermediate areas between the outside edge of broad ring and the inner wall of the glass dish as is shown in Fig. 3e to h. The similar patterns were

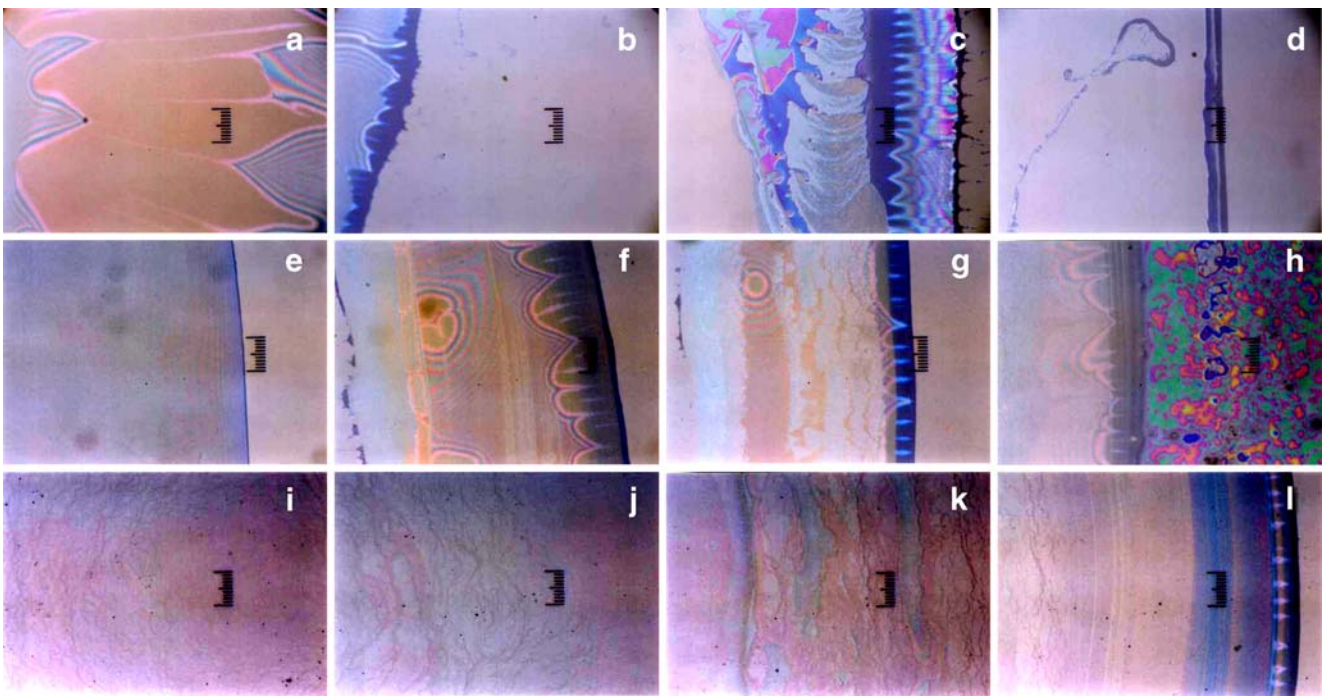

Fig. 4 Microscopic drying patterns of CS1000A (1)+CS300 (2)+CS161 (3) mixtures in a watch glass (**a** to **d**), a glass dish (**e** to **h**), and a cover glass (**i** to **l**) at 24 °C. $\phi_1=\phi_2=\phi_3=0.00229$, from center (**a**, **e**, **i**) to the right edge (**d**, **h**, **l**), full scale is 0.2 mm

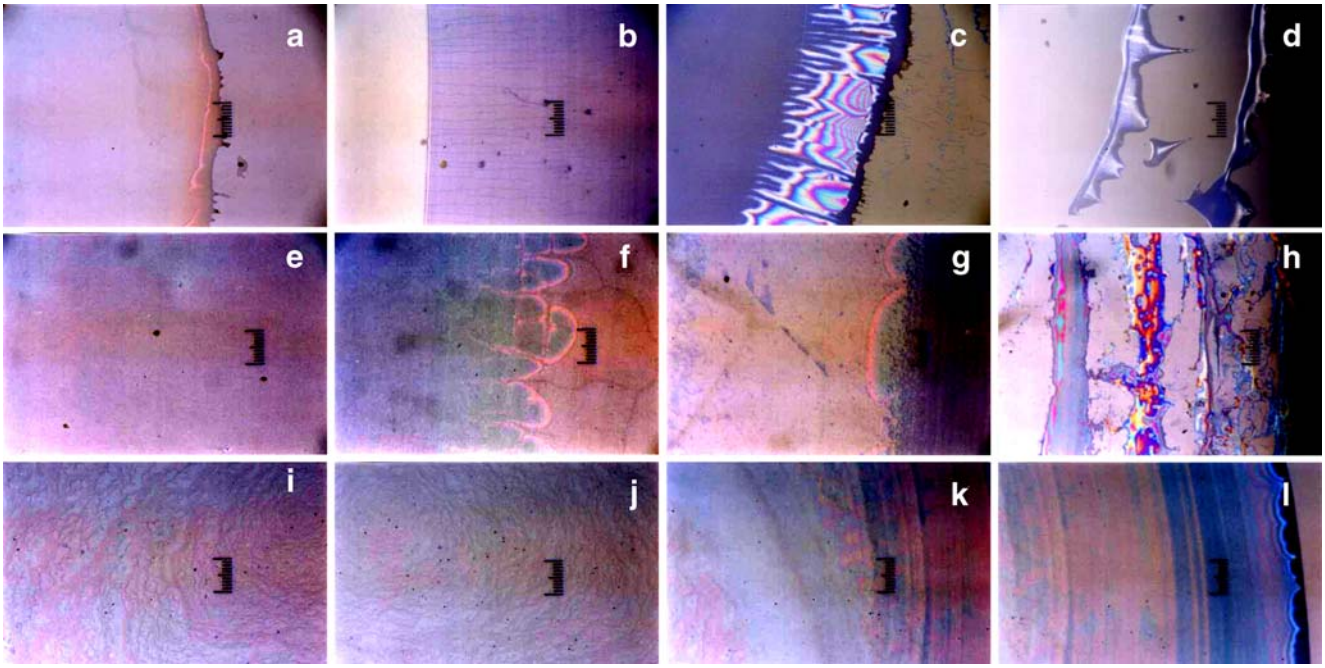

Fig. 5 Microscopic drying patterns of CS1000A (1)+CS300 (2)+CS161 (3) mixtures in a watch glass (**a** to **d**), a glass dish (**e** to **h**) and a cover glass (**i** to **l**) at 24 °C. $\phi_1=\phi_2=\phi_3=0.0069$, from center (**a**, **e**, **i**) to the right edge (**d**, **h**, **l**), full scale is 0.2 mm

observed for the diluted suspensions of CS300 spheres for the first time [11]. The drying frontier started at the center of the glass dish and moved toward the outer cell wall with time. These wave-shaped patterns appeared only when the concentration of the spheres is not high enough to covering of the spheres over the cell surfaces.

On a cover glass, rather sharp two or three broad rings were formed at the middle and outside areas of the dried films (see Fig. 3i to l). The outside broad rings were always bluish and iridescent colored. It should be mentioned here that the whole area except the broad rings were blue. The film thickness profile and AFM measurements clarified that the small and large spheres were segregated effectively to the outside broad ring region and the central area, respectively. The middle size spheres located mainly at the middle broad ring area. However, rather large amount of large spheres also coexisted in the middle area. These incomplete segregation effects for the ternary mixtures will be discussed again in the "Microscopic drying patterns of ternary sphere mixtures" section below.

Microscopic drying patterns of ternary sphere mixtures

Figures 4 and 5 show the typical examples of the microscopic drying patterns of the ternary mixtures in a watch glass, a glass dish and a cover glass and at $\phi_1=\phi_2=\phi_3=0.00229$ and 0.0069, respectively. On a watch glass in Fig. 4 (a to d) several clear-cut boundaries between the differently iridescent colored layers are observed. Assignment of the layers to the three kinds of spheres is quite difficult, though tendency of the color change from reddish to bluish in the regions from the center to the outside edge is obvious. In a glass dish, very-fine-layered and wave-like patterns were observed. On a cover glass, a fine-layered structure is formed especially at the outside region. However, assignment of each layer to the sphere size is again quite difficult except the blue broad ring at the outside edge, which is composed of the small CS161 spheres. It should be mentioned here that the boundaries in a watch glass were observed clearly in Fig. 5 a to d compared with those shown in Fig. 4 a to d. This supports that the segregation effect takes place more effectively at the higher sphere concentrations.

Figure 6 shows the reflection spectra of the dried films of CS1000A+CS300+CS161 on a watch glass. The spectra

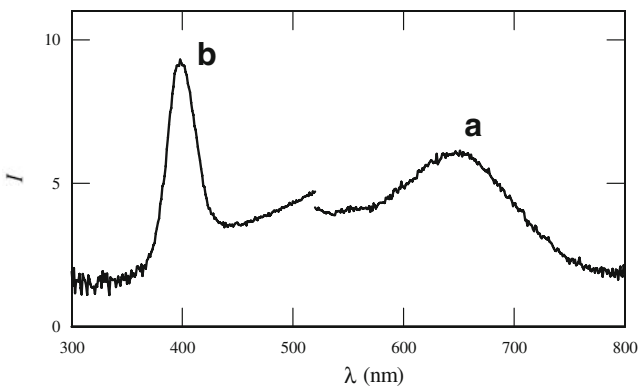

Fig. 6 Reflection spectra of the dried films of CS1000A (1)+CS300 (2)+CS161 (3) mixtures in a watch glass at 24 °C. Code 454, $\phi=0.0128$, **a** middle layer, **b** outer layer

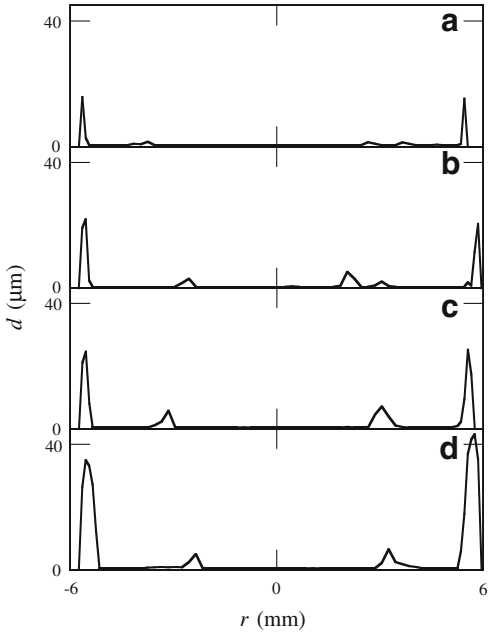

Fig. 7 The thickness profiles of the dried film (d) of the ternary sphere mixtures CS1000A (1)+CS300 (2)+CS161 (3) as a function of the distance from the pattern center (r) at 25 °C. $\phi_1=\phi_2=\phi_3=$**a** 0.00229, **b** 0.0046, **c** 0.0069, **d** 0.0128

a and b are those at the middle and outer layers, and the peak wavelengths (λ_p) are 655 nm and 400 nm, respectively. The nearest-neighbored intersphere distance (D) is estimated from the peak wavelengths (λ_p) using Eq. 1 [51]:

$$D = 0.6124(\lambda_p/n) \quad (1)$$

Here, the refractive index of the dried film (n) is given by Eq. 2.

$$n = 0.74 \times [\text{refractive index of silica}] + 0.26 \times [\text{refractive index of air}] \quad (2)$$

Refractive indices of silica and air were assumed to be 1.5 and 1.00, respectively. Furthermore, the spheres in the dried film are assumed to be attached to each other and distribute in the closed-packed colloidal crystal structure. The D values of the dried film were evaluated to be 284 nm and 173 nm, respectively. These values agreed excellently with the diameters of CS300 and CS161 spheres, 305 nm and 183 nm, respectively. This agreement supports that the neighbored spheres are almost in contact with each other, keeping a close-packed structure. Thus, the peak wave-

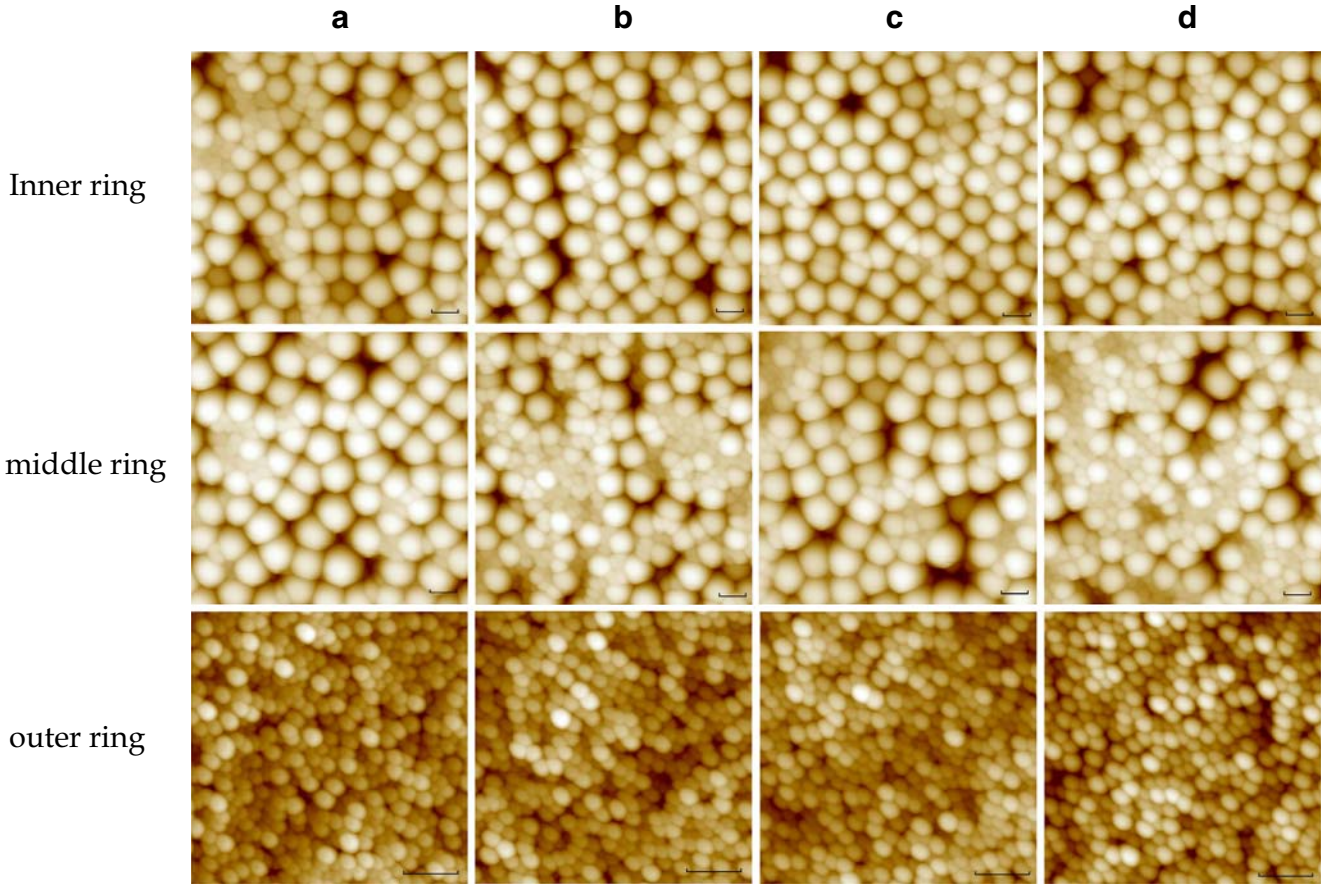

Fig. 8 AFM images of the dried films of CS1000A (1)+CS300 (2)+CS161 (3) mixtures at the inner ring area, middle and outside areas from the top on a cover glass. Sphere concentration: from the left column, $\phi_1=\phi_2=\phi_3=0.00229$ (**a**), 0.0046 (**b**), 0.0069 (**c**), and 0.0128 (**d**). Scan size: from the top line, 10 μm×10 μm, 10 μm×10 μm, and 5 μm×5 μm. Length of the bars is 1 μm

lengths at 655 nm and 400 nm are attributed to the colloidal crystal films of CS300 and CS161 spheres, respectively. It should be mentioned here that the primary and secondary peak wavelengths corresponding to the crystal structure of CS1000A spheres are estimated to be 2,630 nm and 1,315 nm, respectively, which are highly beyond the wavelength range measurable, i.e., 300 nm to 900 nm. Thus, no observation of the peak profiles of CS1000A crystals in this work is quite reasonable.

Figure 7 shows the thickness profiles of the dried film for CS1000A+CS300+CS161 mixtures on a cover glass. The sharp broad ring composed of small CS161 spheres appeared at the outside edge. The heights of the broad rings increased proportionally as sphere concentration increased. However, distinct broad rings corresponding medium and large spheres were not observed in the figures. For the binary mixtures, coexistence of the rather sharp principal broad rings and the low and wide ones was clear at the outside edge and the inner area, respectively [48]. These results support that the size-segregation effect for the small spheres is strong, but that for the medium and large spheres is weak on a cover glass.

Figure 8 shows the AFM observation of the air–film interface of the dried films of the ternary mixtures on a cover glass. Surprisingly, the size-segregation effect for the large and small spheres toward the inner and the outside regions is very clear as the authors expected before the observation. As is clearly seen in the figure, segregation effect for the medium spheres was not so clear at the middle region, and the coexistence of large and medium spheres were observed, which is consistent with the macroscopic observation.

Summarizing the results, colorful three layered drying patterns were observed for the ternary mixtures of colloidal silica spheres having different sizes, 183 nm, 305 nm, and 1.205 μm. The patterns were composed of the outer, middle, and inner layers of small, medium, and large spheres, respectively. In a glass dish, size segregation did not take place so effectively. On a cover glass, size segregation took place, i.e., small, medium, and large spheres located at the outer, medium, and central areas. However, segregation effect on a cover glass was not so complete compared with that on a watch glass.

Acknowledgments Financial supports from the Ministry of Education, Culture, Sports, Science and Technology, Japan and Japan Society for the Promotion of Science are greatly acknowledged for Grants-in-Aid for Exploratory Research (17655046) and Scientific Research (B) (18350057 and 19350110), respectively. Catalysts and Chemicals Co. is thanked deeply for his providing the colloidal silica sphere samples used in this work.

References

1. Terada T, Yamamoto R, Watanabe T (1934) Proc Imper Acad Tokyo 10:10
2. Terada T, Yamamoto R, Watanabe T (1934) Sci Paper Inst Phys Chem Res Jpn 27:75
3. Terada T, Yamamoto R (1935) Proc Imper Acad Tokyo 11:214
4. Ball P (1999) The self-made tapestry formation in nature. Oxford Univ Press, Oxford
5. Fischer BJ (2002) Langmuir 18:60
6. Okubo T, Kimura H, Kimura T, Hayakawa F, Shibata T, Kimura K (2005) Colloid Polymer Sci 283:1
7. Okubo T (2006) Colloid Polymer Sci 285:225
8. Okubo T (2006) Colloid Polymer Sci 284:1395
9. Okubo T (2006) Colloid Polymer Sci 284:1191
10. Okubo T (2006) Colloid Polymer Sci 285:331
11. Okubo T, Okamoto J, Tsuchida A (2007) Colloid Polymer Sci 285:967
12. Okubo T (2007) Colloid Polymer Sci 285:1495
13. Vanderhoff JW, Bladford EB, Carrington WK (1973) J Polymer Sci Symp 41:155
14. Nicolis G, Prigogine I (1977) Self-organization in non-equilibrium systems. Wiley, New York
15. Cross MC, Hohenberg PC (1993) Rev Modern Phys 65:851
16. Adachi E, Dimitrov AS, Nagayama K (1995) Langmuir 11:1057
17. Ohara PC, Heath JR, Gelbart WM (1998) Langmuir 14:3418
18. Uno K, Hayashi K, Hayashi T, Ito K, Kitano H (1998) Colloid Polymer Sci 276:810
19. Gelbart WM, Sear RP, Heath JR, Chang S (1999) Faraday Discuss Chem Soc 112:299
20. van Duffel B, Schoonheydt RA, Grim CPM, De Schryver FC (1999) Langmuir 15:957
21. Maenosono S, Dushkin CD, Saita S, Yamaguchi Y (1999) Langmuir 15:957
22. Brock SL, Sanabria M, Suib SL, Urban V, Thiyagarajan P, Potter DI (1999) J Phys Chem 103:7416
23. Nikoobakht B, Wang ZL, El-Sayed MA (2000) J Phys Chem 104:8635
24. Ge G, Brus L (2000) J Phys Chem 104:9573
25. Chen KM, Jiang X, Kimerling LC, Hammond PT (2000) Langmuir 16:7825
26. Lin XM, Jaenger HM, Sorensen CM, Klabunde KJ (2001) J Phys Chem 105:3353
27. Kokkoli E, Zukoski CF (2001) Langmuir 17:369
28. Ung T, Liz-Marzan LM, Mulvaney P (2001) J Phys Chem 105:3441
29. Haw MD, Gilli M, Poon WCK (2002) Langmuir 18:1626
30. Narita T, Beauvais C, Hebrand P, Lequeux F (2004) Eur Phys J E 14:287
31. Tirumkudulu MS, Russel WB (2005) Langmuir 21:4938
32. Shimomura M, Sawadaishi T (2001) Curr Opinion Colloid Interf Sci 6:11
33. Okubo T, Okuda S, Kimura H (2002) Colloid Polymer Sci 280:454
34. Okubo T, Kimura K, Kimura H (2002) Colloid Polymer Sci 280:1001
35. Okubo T, Kanayama S, Ogawa H, Hibino M, Kimura K (2004) Colloid Polymer Sci 282:230
36. Okubo T, Kanayama S, Kimura K (2004) Colloid Polymer Sci 282:486
37. Okubo T, Yamada T, Kimura K, Tsuchida A (2005) Colloid Polymer Sci 283:1007

38. Yamaguchi T, Kimura K, Tsuchida A, Okubo T, Matsumoto M (2005) Colloid Polymer Sci 283:1123
39. Kimura K, Kanayama S, Tsuchida A, Okubo T (2005) Colloid Polymer Sci 283:898
40. Okubo T, Shinoda C, Kimura K, Tsuchida A (2005) Langmuir 21:9889
41. Okubo T, Yamada T, Kimura K, Tsuchida A (2006) Colloid Polymer Sci 284:396
42. Okubo T, Itoh E, Tsuchida A, Kokufuta E (2006) Colloid Polymer Sci 285:339
43. Okubo T, Nozawa M, Tsuchida A (2007) Colloid Polymer Sci 285:827
44. Okubo T, Kimura K, Tsuchida A (2007) Colloids Surfaces 56:201
45. Okubo T, Onoshima D, Tsuchida A (2007) Colloid Polymer Sci 285:999
46. Okubo T, Nakagawa N, Tsuchida A (2007) Colloid Polymer Sci 285:1247
47. Okubo T, Yokota N, Tsuchida A (2007) Colloid Polymer Sci 285:1257
48. Okubo T, Kimura K, Tsuchida A, Colloid Polymer Sci., in press. (DOI 10.1007/s00396-007-1778-6)
49. Okubo T, Kimura K, Tsuchida A, Colloid Polymer Sci., in press. (DOI 10.1007/s00396-007-1808-4), Regulated T & H
50. Erkseliusa S, Wadso L, Karlsson O (2007) Colloid Polymer Sci 285:1707
51. Okubo T (1986) J Chem Soc Faraday Trans 1 82:3175